

Hydrogen Evolution Catalyzed by an Iron Polypyridyl Complex in Aqueous Solutions

G. P. Connor,[†] K. J. Mayer,[†] C. S. Tribble,[†] and W. R. McNamara^{*,†}[†]Department of Chemistry, College of William and Mary, PO Box 8795, Williamsburg, Virginia 23187-8795, United States

Supporting Information

ABSTRACT: Iron complexes containing tetradentate monophenolate ligands have been found to be highly active for the electrocatalytic reduction of protons to hydrogen gas. Catalysis occurs at -1.17 V vs SCE in CH_3CN with a turnover frequency of up to 1000 s^{-1} and a 660 mV overpotential. Interestingly, the catalyst activity is enhanced in the presence of water, achieving turnover frequencies of 3000 s^{-1} with an overpotential of 800 mV, making it one of the most active iron electrocatalysts currently reported. The catalyst is also capable of generating hydrogen from purely aqueous buffer solutions of pH 3–5 with Faradaic efficiencies of 98%.

Developing systems for artificial photosynthesis (AP) is a promising method for harnessing solar energy.¹ In general, systems for AP split water to give oxygen (water oxidation) and hydrogen (proton reduction). Generating hydrogen gas from aqueous protons is essential toward developing integrated systems for AP.¹ Furthermore, the development of robust electrocatalysts for proton reduction is a critical step toward developing a system for total overall water splitting.

Although platinum can be used to reduce protons to hydrogen gas, the rare nature of this metal limits the widespread application of platinum in devices for AP. To this end, several cobalt and nickel complexes have been examined that are active hydrogen-generation catalysts. Cobalt glyoxime complexes have been widely studied and can be tuned to operate at low overpotential.² These complexes have also been used for photocatalytic hydrogen generation but decompose after hours of irradiation.³ Phosphine complexes of cobalt and nickel also catalyze proton reduction at low overpotential with turnover frequencies (TOFs) as high as 10^5 s^{-1} .⁴ In order to improve stability, polypyridyl ligands have been bound to cobalt and molybdenum to generate hydrogen from aqueous solutions.⁵ Although cobalt, nickel, and molybdenum are more abundant than platinum, it is of great interest to develop catalysts that contain the most abundant transition metal, iron.

With structural elucidation of iron-only and NiFe hydrogenases, there has been much effort into synthesizing mimics of the $\text{Fe}_2(\mu\text{-SR})_2(\text{CN})_2(\text{CO})_3\text{L}_n$ (where $\text{L}_n = \text{H}_2\text{O}/\text{H}_2$) active site of the enzyme.⁶ Model complexes have been found to electrocatalytically generate hydrogen with the addition of an acid in organic solvents at potentials more cathodic than -1.2 V vs SCE.⁶ Although these bioinspired systems were observed to be active electrocatalysts, they are far less active than what is observed for $[\text{Fe}]_2\text{H}_2\text{ase}$ and are catalytic at fairly negative

potentials.⁷ There are other recent examples of iron catalysts that are only active in nonaqueous media.^{7b,8} Examples of iron electrocatalysts that operate in aqueous media are more limited and either are active over a narrow pH range or operate at very cathodic potentials (less than -1.4 V vs SCE).⁹ Recently, iron carbonyl clusters have been reported that evolve hydrogen at -1.25 V vs SCE in aqueous solutions at pH 5 with $k_{\text{obs}} \sim 700$ s^{-1} .^{8c,9d} Currently, there are no examples of mononuclear iron electrocatalysts that both are highly active and operate at modest potentials in aqueous solutions. Herein we report a mononuclear iron polypyridyl catalyst that is active in aqueous solutions and achieves TOFs of up to 3000 s^{-1} at -1.17 V vs SCE.

Tetradentate monophenolate ligands have been used to model multiple iron-containing enzymes but have not been examined for the purpose of proton reduction catalysis.¹⁰ These complexes are stable in water, and cyclic voltammograms (CVs) of these complexes show reversible $\text{Fe}^{\text{III}}/\text{Fe}^{\text{II}}$ reductions between -0.1 and -0.63 V vs NHE.¹¹ The ligands also formed iron complexes that were both air- and water-stable. Therefore, we reasoned that these complexes are promising candidates for hydrogen-generation catalysis.

Ligand synthesis proceeds through a modified literature procedure to give ligand **1** in good yield (59%).¹¹ The ligand was deprotonated by triethylamine and coordinated to FeCl_3 in methanol. X-ray-quality crystals were obtained through slow diffusion in dichloromethane/diethyl ether ($R_1 = 0.0487$, P_2/n). Figure 1 shows the structure of **1** as a distorted octahedral complex. The O–Fe–N and N–Fe–Cl bond angles of 162.08° , 167.23° , and 166.99° delineate from the expected values of 180° for an octahedral coordination sphere. The Fe–O bond of 1.896

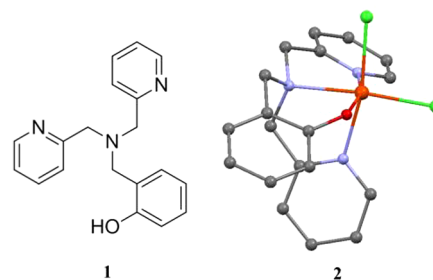


Figure 1. Left: Tetradentate monophenolate ligand (**1**). Right: Iron catalyst (**2**). Color code: iron, orange; oxygen, red; chlorine, green; nitrogen, blue; carbon, black. Hydrogen atoms have been omitted for clarity.

Received: January 13, 2014

Published: May 21, 2014

\AA is shorter than other reported iron(III) phenolate bonds reported in the literature.¹²

CVs of the catalyst were obtained upon the addition of known concentrations of trifluoroacetic acid (TFA) in acetonitrile (Figure 2). Upon the addition of acid, an irreversible reduction

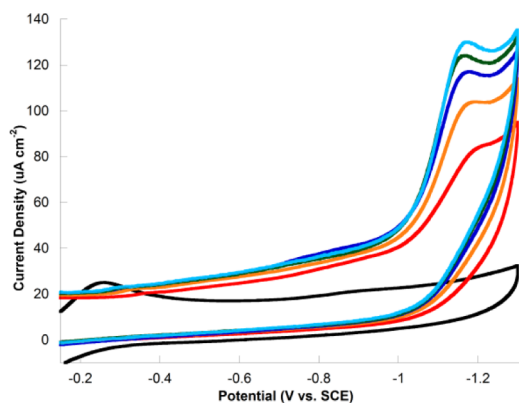


Figure 2. CVs of 0.5 mM **2** in CH_3CN with 0.1 M TBAPF_6 (black) upon the addition of 2.2 mM TFA (red), 4.4 mM TFA (orange), 6.6 mM TFA (dark blue), 8.8 mM TFA (green), and 11.0 mM TFA (light blue) at a scan rate of 200 mV s^{-1} with a glassy carbon working electrode.

event is observed at -1.17 V vs SCE, suggesting that catalysis occurs with a 660 mV overpotential in CH_3CN . When more acid is added, a larger current enhancement is observed.

The linear relationship between i_c and $[\text{TFA}]$ suggests a second-order dependence on the proton concentration (see the Supporting Information, SI). Decomposition of the catalyst occurs at a high acid concentration, leading to deviation from linearity at these concentrations. The catalyst is highly active for an iron complex with $i_c/i_p = 7.8$ in CH_3CN (see Figure S1 in the SI). This corresponds to a TOF of 1000 s^{-1} . This compares favorably with fluorinated iron oxime complexes that also produce $i_c/i_p = 8$ in organic media.^{7b}

Although the catalyst is highly active in an organic solution, our goal is to develop a catalyst that can reduce protons in aqueous solutions. To this end, the CVs of the catalyst in 1:1 $\text{CH}_3\text{CN}/\text{H}_2\text{O}$ solutions upon the addition of TFA were obtained. Similar to the experiments in CH_3CN , a catalytic wave is observed at a potential more cathodic than the $\text{Fe}^{\text{III}}/\text{Fe}^{\text{II}}$ reduction (Figure 3),

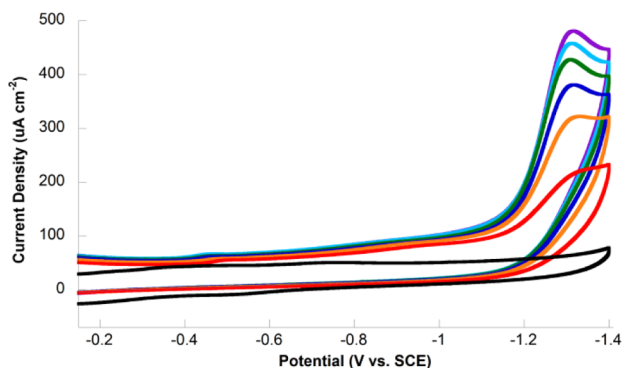


Figure 3. CVs of 0.5 mM **2** in 1:1 $\text{CH}_3\text{CN}/\text{H}_2\text{O}$ (black) with 0.1 M TBAPF_6 upon the addition of 2.2 mM TFA (red), 4.4 mM TFA (orange), 6.6 mM TFA (blue), 8.8 mM TFA (green), 11.0 mM TFA (light blue), and 13.2 mM TFA (purple) at a scan rate of 200 mV s^{-1} with a glassy carbon working electrode.

corresponding to an overpotential of 800 mV for the catalyst in this solvent mixture. A linear relationship between $[\text{TFA}]$ and i_c is also observed in the acetonitrile/water solution, indicating a second-order relationship with the proton concentration, as seen in the purely organic solvent. At high acid concentration ($[\text{TFA}] > 30 \text{ mM}$), catalyst decomposition is observed, resulting in a nonlinear i_c versus $[\text{TFA}]$ relationship. Interestingly, the catalyst is much more active in the presence of water. In these solvent conditions, an $i_c/i_p = 11.9$ is observed, corresponding to a TOF of 3000 s^{-1} (see Figure S15 in the SI). The TOFs were calculated using the following expression:⁴

$$\frac{i_{\text{cat}}}{i_p} = \frac{n}{0.4463} \sqrt{\frac{RTk_{\text{obs}}}{F\nu}} \quad (1)$$

It is important to note that a scan rate of 10 V s^{-1} was used to obtain values for the TOF. At scan rates greater than 10 V s^{-1} , no increase in i_c was observed (Figure S24 in the SI). This suggests that at $\nu = 10 \text{ V s}^{-1}$ the catalytic process is not diffusion-controlled and eq 1 can be used to calculate the TOF.⁴ Although eq 1 accurately represents simple pseudo-first-order systems, it is also used to determine TOFs for more complicated systems in order to provide a point of comparison for different catalysts.^{4c,5b,c,8c}

Upon the addition of TFA, a large current enhancement is observed at a potential that is more negative than that of the reversible redox couple for $\text{Fe}^{3+}/\text{Fe}^{2+}$. It must also be noted that the $\text{Fe}^{3+}/\text{Fe}^{2+}$ redox couple shifts to a more positive potential (0.1 V vs SCE; see Figure S6 in the SI) once acid is added. This suggests that the oxygen of the phenolate is likely protonated followed by the reduction of Fe^{III} to Fe^{II} and subsequent reduction and protonation events. This would suggest that catalysis proceeds through either CEEC or a CECE mechanism. When $[\text{TFA}]$ is held constant and the catalyst concentration is varied, a linear relationship between $[\text{catalyst}]$ on i_c is observed (Figure 4). This corresponds to a first-order dependence on $[\mathbf{2}]$. Therefore, the overall rate expression can be written as rate = $k[\mathbf{2}][\text{H}^+]^2$.

In aqueous solutions, the electrochemical data display irreversible reduction waves at potentials that are more cathodic than the $\text{Fe}^{3+}/\text{Fe}^{2+}$ couple. The potentials of the waves shift based on the pH, showing a cathodic shift of 60 mV per 1.0 increase in the pH unit (Figure 5).

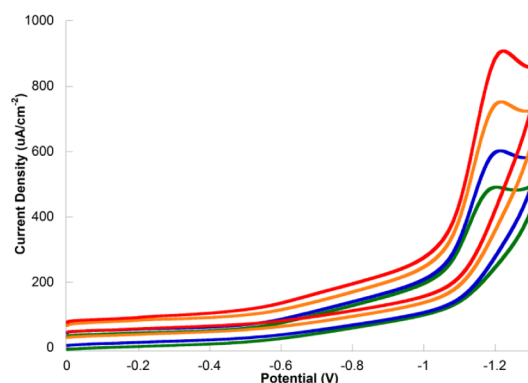


Figure 4. CVs in CH_3CN with 0.1 M TBAPF_6 containing 44 mM TFA with 0.2 mM (green), 0.3 mM (blue), 0.4 mM (orange), and 0.5 mM (red) of **2** at a scan rate of 200 mV s^{-1} with a glassy carbon working electrode.

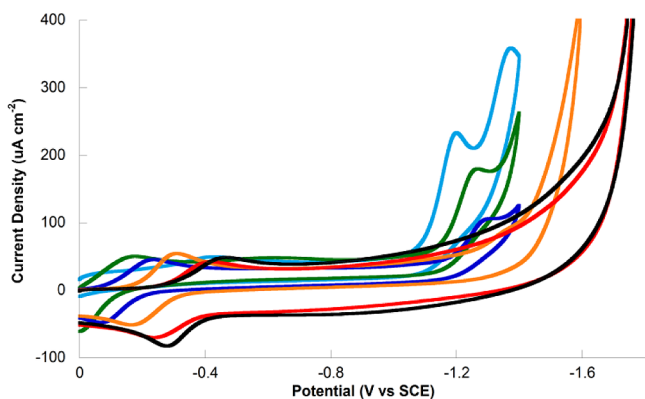


Figure 5. CVs of 0.5 mM **2** in citrate-buffered aqueous solutions at pH 3.0 (light blue), 4.0 (green), 5.0 (blue), 6.0 (orange), 7.0 (red), and 8.0 (black) at a scan rate of 200 mV s^{-1} with a glassy carbon working electrode.

While the CVs obtained in an aqueous buffer help to reinforce the proposed mechanism, it is also of interest to test the catalyst for activity in a purely aqueous solution. Bulk electrolysis was performed at -1.2 V (vs SCE) to confirm that these reduction events correspond to electrocatalytic hydrogen generation. The potential was held at -1.2 V to correspond to the reduction wave observed in the CV of the complex in a buffer solution. In a typical experiment, the working electrode is held at a constant potential and the current is monitored over time. Gas chromatography was used to determine the evolution of hydrogen, and Faradaic efficiencies of 98% were observed for pH 3–5 (see the SI).

An iron complex containing a tetradentate monophenolate ligand has been found to be highly active for the electrocatalytic reduction of protons to hydrogen gas. Catalysis occurs at -1.17 V vs SCE in CH_3CN with a TOF up to 1000 s^{-1} and an overpotential of 660 mV. In the presence of water, the catalyst is stable and highly active with an i_c/i_p of 11.9 and an overpotential of 800 mV, making it one of the most active iron electrocatalysts reported to date (TOF = 3000 s^{-1}). The catalysis is first-order with respect to [catalyst] and second-order with respect to [acid]. The catalyst is also active in purely aqueous solutions. Bulk electrolysis shows that **2** is capable of generating hydrogen from purely aqueous buffer solutions of pH 3–5 with Faradaic efficiencies of 98%.

■ ASSOCIATED CONTENT

Supporting Information

Synthesis, crystallographic data, supplementary figures, experimental details, other materials, and a CIF file. This material is available free of charge via the Internet at <http://pubs.acs.org>.

■ AUTHOR INFORMATION

Corresponding Author

*E-mail: wrmcnamara@wm.edu.

Notes

The authors declare no competing financial interest.

■ ACKNOWLEDGMENTS

W.R.M. thanks Robert D. Pike for assistance with X-ray crystallography. This work was funded by the Virginia Space Grant Consortium New Investigator Award.

■ REFERENCES

- (1) (a) Lewis, N. S.; Nocera, D. G. *Proc. Natl. Acad. Sci. U. S. A.* **2006**, *103*, 15729. (b) Eisenberg, R. *Science* **2009**, *324*, 44.
- (2) Dempsey, J. L.; Brunschwig, B. S.; Winkler, J. R.; Gray, H. B. *Acc. Chem. Res.* **2009**, *42*, 1995.
- (3) (a) Du, P. W.; Knowles, K.; Eisenberg, R. *J. Am. Chem. Soc.* **2008**, *130*, 12576. (b) Lazarides, T.; McCormick, T.; Du, P. W.; Luo, G. G.; Lindley, B.; Eisenberg, R. *J. Am. Chem. Soc.* **2009**, *131*, 9192. (c) McCormick, T. M.; Calitree, B. D.; Orchard, A.; Kraut, N. D.; Bright, F. V.; Detty, M. R.; Eisenberg, R. *J. Am. Chem. Soc.* **2010**, *132*, 15480. (d) Probst, B.; Rodenberg, A.; Guttentag, M.; Hamm, P.; Alberto, R. *Inorg. Chem.* **2010**, *49*, 6453. (e) Fihri, A.; Artero, V.; Razavet, M.; Leibl, W.; Fontecave, M. *Angew. Chem.* **2008**, *47*, 564–567. (f) Hawacker, J.; Lehn, J. M.; Ziessel, R. *New J. Chem.* **1983**, *7*, 271–277.
- (4) (a) Wilson, A. D.; Newell, R. H.; McNevin, M. J.; Muckerman, J. T.; Rawoski-Dubois, M.; Dubois, D. L. *J. Am. Chem. Soc.* **2006**, *128*, 358. (b) Rakowski-Dubois, M.; Dubois, D. L. *Acc. Chem. Res.* **2009**, *42*, 1974. (c) Helm, M. L.; Stewart, M. P.; Bullock, R. M.; Rawkowski-Dubois, M.; Dubois, D. L. *Science* **2011**, *333*, 863. (d) Hoffert, W. A.; Roberts, J. A. S.; Bullock, R. M.; Helm, M. L. *Chem. Commun.* **2013**, *49*, 7767–7769.
- (5) (a) Sun, Y.; Bigi, J. P.; Piro, N. A.; Tang, M. L.; Long, J. R.; Chang, C. J. *J. Am. Chem. Soc.* **2011**, *133*, 9212. (b) Bigi, J. P.; Hanna, T. E.; Harman, W. H.; Chang, A.; Chang, C. J. *Chem. Commun.* **2010**, *46*, 958. (c) Sun, Y. J.; Sun, J. W.; Long, J. R.; Yang, P. D.; Chang, C. J. *Chem. Sci.* **2013**, *4*, 118. (d) Karunadasa, H. L.; Chang, C. J.; Long, J. R. *Nature* **2010**, *464*, 1329–1333. (e) Stubbert, B.; Peters, J. C.; Gray, H. B. *J. Am. Chem. Soc.* **2011**, *133*, 9212. (f) Singh, W. M.; Mirmohades, M.; Jane, R. T.; White, T. A.; Hammarstrom, L.; Thapper, A.; Lomoth, R.; Ott, S. *Chem. Commun.* **2013**, *49*, 8638.
- (6) (a) Garcin, E.; Vernede, X.; Hatchikian, E. C.; Volbeda, A.; Frey, M.; Fontecilla-Camps, J. C. *Structure* **1999**, *7*, 557–566. (b) Peters, J. W.; Lanzilotta, W. N.; Lemon, B. J.; Seefeldt, L. C. *Science* **1998**, *282*, 1853–1858. (c) Zhao, X.; Georgakaki, I. P.; Miller, M. L.; Yarbrough, J. C.; Darensbourg, M. Y. *J. Am. Chem. Soc.* **2001**, *123*, 9710–9711. (d) Felton, G. A. N.; Glass, R. S.; Lichtenberger, D. L.; Evans, D. H. *Inorg. Chem.* **2006**, *45*, 9181–9184. (e) Gloaguen, F.; Lawrence, J. D.; Rauchfuss, T. B. *J. Am. Chem. Soc.* **2001**, *123*, 9476–9477.
- (7) (a) Adams, M. W. W. *Biochim. Biophys. Acta* **1990**, *1020*, 115–145. (b) Rose, M. J.; Gray, H. B. *J. Am. Chem. Soc.* **2012**, *134*, 8310. (c) Artero, V.; Fontecave, M. *Coord. Chem. Rev.* **2005**, *249*, 1518–1535.
- (8) (a) Kaur-Ghuman, S.; Schwartz, L.; Lomoth, R.; Stein, W.; Ott, S. *Angew. Chem., Int. Ed.* **2010**, *49*, 8033. (b) Bhugun, I.; Lexa, D.; Saveant, J.-M. *J. Am. Chem. Soc.* **1996**, *118*, 3982. (c) Nguyen, A. D.; Rail, M. D.; Shanmugam, M.; Fetting, J. C.; Berben, L. A. *Inorg. Chem.* **2013**, *52*, 12847–12854.
- (9) (a) Le Cloirec, A.; Davies, S. C.; Evans, D.; Hughes, D. L.; Pickett, C. J.; Best, S. P.; Borg, S. *Chem. Commun.* **1999**, 2285. (b) Singleton, M. L.; Reibenspies, J. H.; Darensbourg, M. Y. *J. Am. Chem. Soc.* **2010**, *132*, 8870. (c) Quentel, F.; Passard, G.; Gloaguen, F. *Energy Environ. Sci.* **2012**, *5*, 7757. (d) Rail, M. D.; Berben, L. A. *J. Am. Chem. Soc.* **2011**, *133*, 18577–18579.
- (10) Costas, M.; Mehn, M. P.; Jensen, M. P.; Que, L., Jr. *Chem. Rev.* **2004**, *104*, 939–986.
- (11) Mayilmurugan, R.; Visvaganesan, K.; Suresh, E.; Palaniandavar, M. *Inorg. Chem.* **2009**, *48*, 8771–8783.
- (12) Viswanathan, R.; Palaniandavan, M.; Blasubramanian, T.; Muthiah, P. T. *Inorg. Chem.* **1998**, *37*, 2943–2951.